The effect of heat treatment on sliding wear behaviour of a zinc-based alloy containing nickel and silicon

B.K. Prasad

Regional Research Laboratory, Bhopal-462026, India

Received 12 January 2003; accepted 21 April 2003

This investigation deals with the observations made pertaining to the sliding wear behaviour of a zinc-based alloy containing nickel and silicon in partially lubricated condition. Wear tests were conducted over a range of applied pressures and sliding speeds. The effect of microstructural changes brought about through T6 heat treatment involving solutionizing followed by artificial ageing on wear behaviour was also investigated. The wear rate increased with pressure. The slope of the wear rate versus pressure plots was low initially up to a specific pressure. This was followed by a higher slope beyond the (specific) pressure. In some cases, the rate of change in wear rate, i.e. the slope, decreased at still higher pressures. Moreover, the (specific) pressure decreased with sliding speed in general. Increasing sliding speed caused the wear rate of the as-cast zinc-based alloy to increase up to a sliding speed of 2.68 m/s. The trend reversed at a still higher speed of 4.60 m/s. However, increasing wear rate with speed was noted for the heat-treated alloy over the entire speed range. Heat treatment led to reduced wear rate up to a sliding speed of 2.68 m/s. An opposite trend was observed at a higher speed of 4.60 m/s in this case. Specimen seizure was noted at speeds above 2.68 m/s in the case of the as-cast alloy whereas seizure took place only at 4.60 m/s for the heat-treated alloy samples. Frictional heating increased with pressure and speed. The specific response and changing mode of distribution of various phases were thought to be responsible for the typical wear behaviour of the alloy in specific material and test conditions. The predominance of parameters like thermal stability and cracking tendency over each other is suggested to lead to the varying wear behaviour of the alloy in different (material and sliding) conditions. The wear response of the samples has been substantiated through characteristics of their wear surfaces, subsurface regions and debris.

KEY WORDS: mixed lubrication, sliding wear behaviour, heat treatment, microstructure-wear property correlations

1. Introduction

Zinc-based alloys have been observed to have potential to substitute various ferrous and non-ferrous alloys [1–3]. The "high strength" variety of the zinc-based alloy system containing 8–28% Al, 1–3% Cu, and ~0.05% Mg has found a place in a variety of engineering applications [1–3]. However, it suffers from shortcomings like inferior elevated temperature properties [1–3] and dimensional instability [4,5]. Heat treatment and reducing the copper content of the alloy system to below 1% have been observed to reduce the problem of dimensional instability [4,5], while partial replacement of copper with high melting elements forming thermally stable microconstituents has led to improved elevated temperature properties. Addition of elements like nickel and/or silicon to the (zinc-based) alloy system has been found to be beneficial in this context [6–9]. In recent studies, the effects of alloying zinc-based alloys with nickel and silicon separately or in combination on dry sliding wear response have been investigated. It has been found that the silicon and/or nickel-containing zinc-based alloys exhibit superior performance under specific test conditions [8,10–14]. However, no information seems to exist pertaining to the effect of heat treatment on the wear behaviour of zinc-based alloys containing nickel and silicon together. Information available on these lines could be quite useful towards more effectively understanding the wear performance of the zinc-based alloys in various material and test conditions and assessing the working capability of the alloy system.

In view of the above, an attempt has been made to study the effects of microstructural changes due to heat treatment on the wear behaviour of a silicon and nickel-containing zinc-based alloy at varying sliding speeds and applied pressures in partially lubricated condition. The study gains importance from the fact that majority of tribological applications, for which the (zinc-based) alloy system has found its suitability on an economic basis, involve sliding of components in sparsely/intermittently lubricated conditions wherein the occurrence of mixed lubrication is very much probable. Moreover, the components operating even in fully lubricated conditions are likely to encounter a partially/mixed lubrication situation during the start and completion of sliding.

2. Experimental

2.1. Alloy preparation

The zinc-based alloy having 27.5% Al, 1.0% Cu, 1.0% Si, 0.9% Ni, 0.03% Mg, and the balance zinc was

1023-8883/03/1000–0333/0

prepared by the liquid metallurgy route. Cast iron moulds were used to solidify the alloy melt in the form of 20 mm diameter, 150 mm long cylindrical rods.

2.2. Heat treatment

The alloy castings were solutionized at 370 °C for 10 h followed by ageing at 180 °C for 8 h. The samples were quenched in water after solutionizing and ageing. An electrical resistance furnace was used for heat-treating the alloy.

2.3. Microstructural studies and hardness measurement

Microstructural characterization of the as-cast and heat-treated alloy was carried out on 20 mm diameter, 15 mm thick samples. The specimens were prepared metallographically and etched with diluted aqua regia for their microstructural studies. A Leitz (Germany) optical microscope was used for carrying out the microstructural analysis. Hardness measurement was carried out on metallographically polished samples at an applied load of 30 kg using a Vickers' hardness tester.

2.4. Wear tests

Wear tests were carried out on 8 mm diameter, 53 mm long samples (pins) using a Cameron-Plint (U.K.) pin-on-disc machine (figure 1) in the presence of SAE 30 oil with a kinematic viscosity 100 and 10.5 mm^2/s at 40 and 100 °C respectively. The disc (counterface) used in this study was an En25 steel (0.3% C, 0.7% Cr, 2.5% Ni, 0.5% Mo, and the balance iron) disc having hardness Rc32.The surface roughness (R_a) of the pin and disc prior to starting the tests was 0.82 μm. A Rank Taylor Hobson (UK) profilometer (RTH Talysurf 6) was employed for measuring the R_a (the arithmetic mean of the departure of the surface roughness profile from the mean line) values using a cut-off length of 0.8 mm. The samples were tested at sliding speeds of 0.42, 2.68, and 4.60 m/s for a predetermined sliding distance of 2500 m. The tests were conducted at pressures up to the operating pressure limit of the wear test apparatus, i.e. 15 MPa, or until the onset of specimen seizure (in terms of burning of the lubricant, substantial adhesion of the specimen material onto the disc and abnormal noise in the pin–disc assembly prior to traversing the fixed sliding distance of 2500 m), whichever occurred earlier. In order to create a partial/mixed lubrication condition during the wear tests, the disc was immersed in the lubricant and rotated at a speed of 2.68 m/s for a period of 5 s to spin the excess (oil) lubricant off the disc prior to conducting the tests. The quantity of the oil lubricant retained on the disc surface was noted to be 49.327 g/m^2. The temperature near the contacting surface of the samples was recorded during the tests by inserting a chromel–alumel thermocouple through a hole in the pin 1.5 mm away from the contacting surface of the sample. The samples were cleaned thoroughly with acetone and weighed using a Mettler microbalance prior to and after the wear tests. The wear rate was computed by a weight-loss technique.

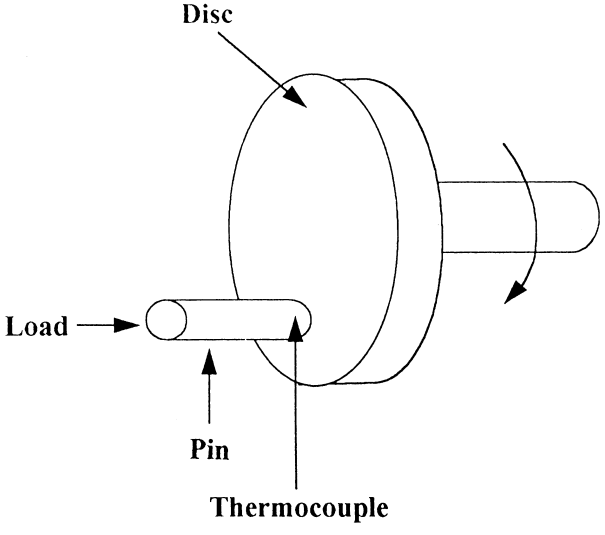

Figure 1. A schematic representation of the pin-on-disc machine.

2.5. Characterization of wear surfaces, subsurface regions and debris

Wear surfaces, subsurface regions and debris particles of typical samples were characterized using a JEOL 35CF scanning electron microscope (SEM). The wear surfaces were mounted on brass studs and sputtered with gold prior to their SEM examination. For the characterization of subsurface regions, longitudinal transverse sections of wear surfaces were mounted in a polyester resin, polished metallographically, etched with diluted aqua regia, mounted on brass studs, sputtered with gold and analyzed using the SEM. The debris particles were suspended in acetone/benzene, spread on a glass slide, fixed on a brass stud using a double-sided tape and sputtered with gold prior to their SEM examination.

3. Results

3.1. Microstructure and hardness

Microstructural features of the alloy in as-cast and heat-treated conditions are shown in figure 2. The as-cast alloy revealed a dendritic structure comprising primary α, eutectoid $\alpha + \eta, \varepsilon$, nickel-containing phase and discrete particles of silicon (figure 2(a) and (b), regions marked by A, B and single, double, and triple arrows respectively). The dendritic structure disappeared and more homogeneous distribution of phases

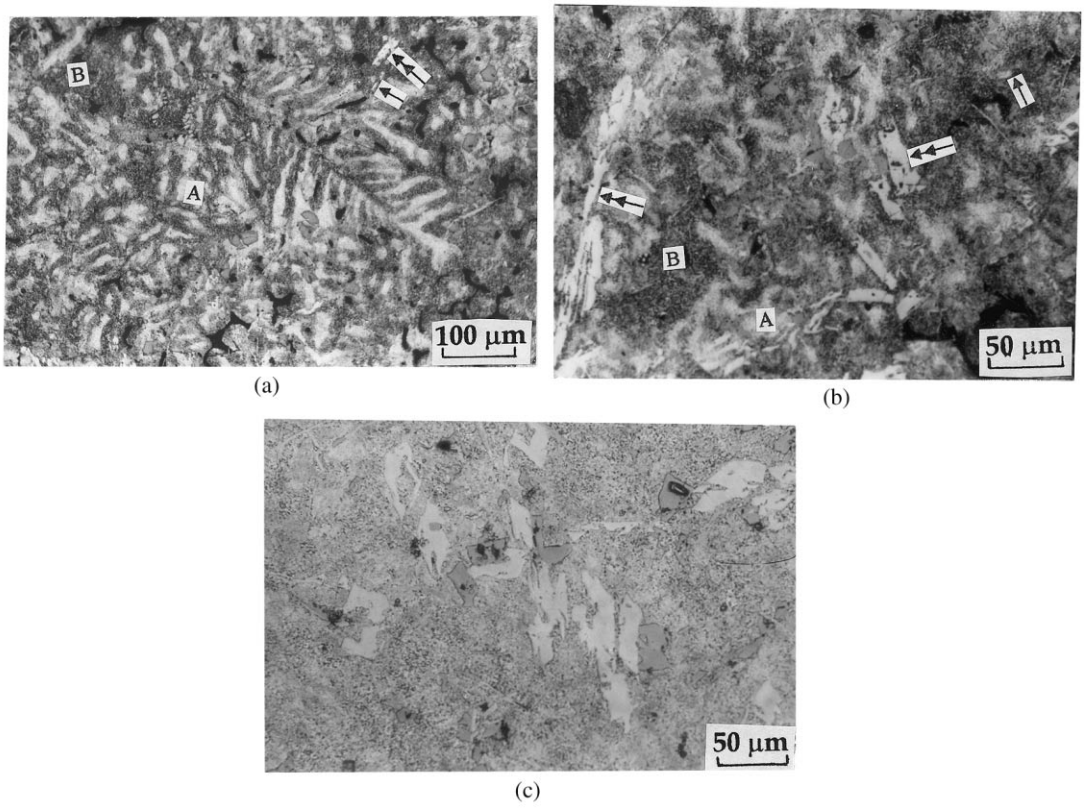

Figure 2. Microstructure of the (a and b) as-cast and (c) heat-treated alloy samples [A: primary α, B: eutectoid $\alpha + \eta$, single arrow: ε, double arrow: nickel-containing phase and triple arrow: silicon particles].

(except silicon particles and nickel-containing constituents) was noted in the heat-treated alloy (figure 2(c)). The hardness of the as-cast alloy was observed to be 145 HV, which reduced to 122 HV as a result of the heat treatment.

3.2. Wear response

Wear rate of the samples has been plotted in figure 3 as a function of applied pressure. The wear rate increased with pressure. The wear rate versus pressure plots attained two slopes in general. The slope was low initially followed by a higher slope beyond a specific pressure. The specific pressure decreased with speed. Sliding speed had a mixed influence on the wear rate of the alloy in as-cast and heat-treated conditions. Increasing sliding speed caused the wear rate of the heat-treated alloy to increase, while this trend was observed up to the speed of 2.68 m/s for the as-cast alloy; the trend reversed beyond the speed in the latter case. The heat-treated alloy attained less wear rate than that of the as-cast one up to a sliding speed of 2.68 m/s. The trend became opposite beyond that speed. Specimen seizure was noted for the as-cast alloy at 2.68 and 4.60 m/s, while this trend was observed at the speed of 4.60 m/s only in the case of the heat-treated samples.

Temperature near the specimen surface has been plotted in figure 4 as a function of test duration. The

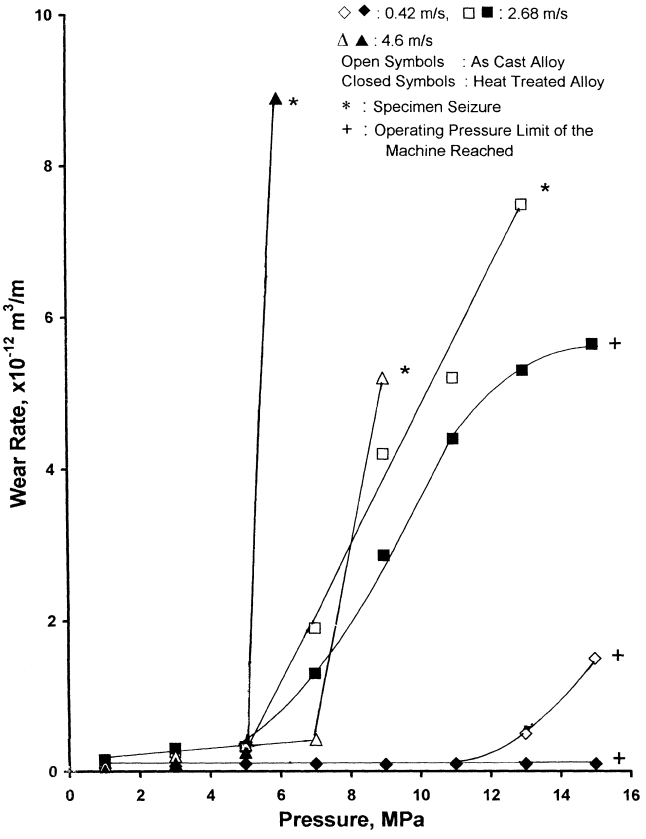

Figure 3. Wear rate of the samples plotted as a function of applied pressure at different speeds.

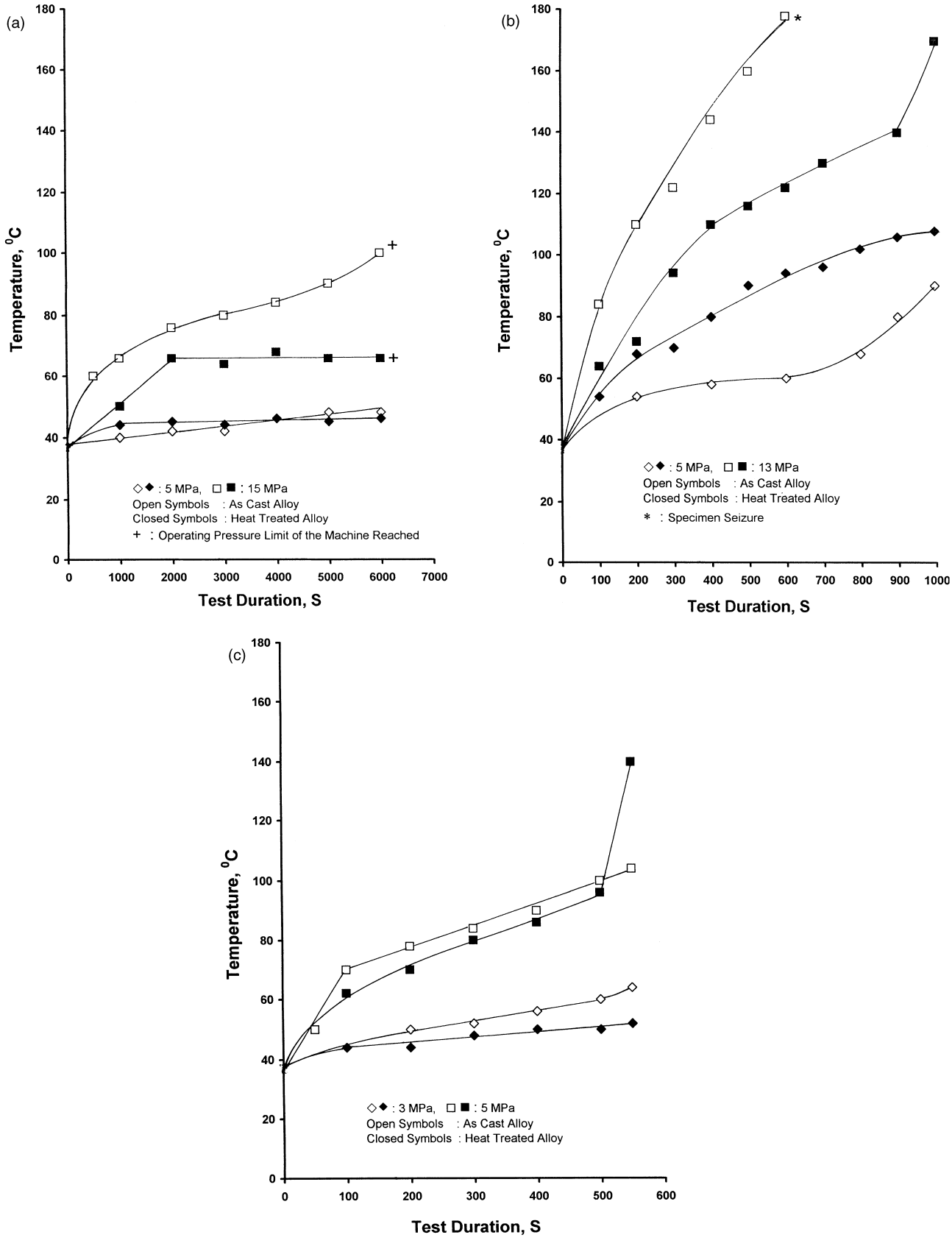

Figure 4. Temperature near the specimen surface plotted as a function of test duration at the sliding speeds of (a) 0.42, (b) 2.68, and (c) 4.60 m/s.

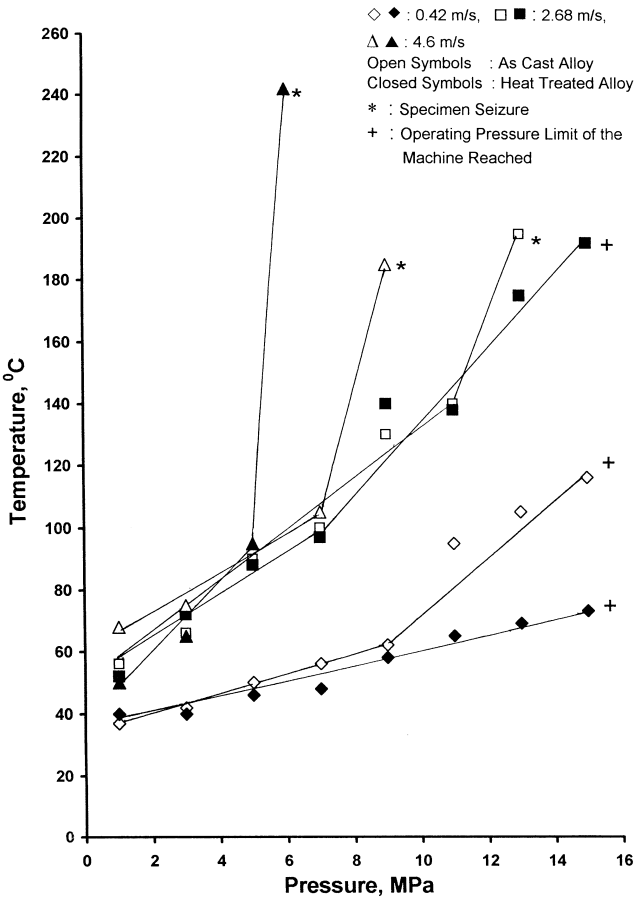

Figure 5. Maximum temperature near the specimen surface plotted as a function of applied pressure at different sliding speeds.

frictional heating increased with the test duration and pressure. The rate of temperature increase was high initially followed by a lower rate of increase at longer durations. This trend was very much prevalent at high speeds (figure 4(b) and (c)). In some cases, the rate of temperature increase was the least in the intermediate test duration (figure 4(b) and (c)).

Maximum temperature near the specimen surface is shown in figure 5 as a function of applied pressure at different speeds. The temperature increased with pressure and speed. Heat-treated samples attained less frictional heating than the as-cast ones at 0.42 m/s, while a mixed effect was noted at higher speeds. The rate of increase in temperature was much higher during specimen seizure.

3.3. Wear surfaces

Figure 6 shows the wear surfaces of the as-cast alloy samples at different speeds and pressures. The wear surfaces were smooth in general at lower speed and pressure with a few deep grooves (figure 6(a), region marked by single arrow). The severity of surface damage increased with pressure (figure 6(b) versus (a), and 6(d) versus (c)) and speed (figure 6(c) versus (a), 6(d) versus (b)). The double-arrow-marked regions in figure 6(b) and (e) show machining chips entrapped on the specimen surface. Sticking of debris on the wear surface was also observed in general (figure 6(a–d)). A magnified view clearly reveals the entrapment/sticking of debris on the wear surface (figure 6(e), regions marked by A). A ripple-like appearance of the wear surface was also observed (figure 6(d)).

3.4. Subsurface regions

Subsurface regions of the as-cast and heat-treated alloy samples are shown in figure 7. The heavily deformed regions comprising extremely fine microconstituents were noted to exist in the nearest vicinity of the wear surface (regions marked by A). A flow of microconstituents (regions marked by B) below the topmost region (marked by A) was noted. This was followed by the presence of the unaffected bulk microstructure (regions marked by C). Microcracking of the nearest vicinity of wear surface was also noted (regions marked by an arrow). A microstructural refinement in the regions close to the wear surface (top) over the one away from the wear surface as well as microcracking of the subsurface regions was observed in the heat-treated alloy (figure 7(e)) similar to the as-cast alloy samples (figure 7(a–d)).

3.5. Wear debris

The debris particles of the as-cast alloy are shown in figure 8. The debris generally comprised flaky particles with a few machining chips (regions marked by A and single arrow respectively). Particles with sharp corners and edges were also observed in the debris (regions marked by double arrow).

4. Discussion

The as-cast alloy comprised a dendritic structure having primary dendrites surrounded by the eutectoid $\alpha + \eta$, ε and nickel and silicon-containing phases (figure 2(a) and (b), regions marked by A, B, and single, double and triple arrows respectively). In other words, preferential distribution of various phases takes place in the as-cast alloy microstructure leading to micro-inhomogeneity in terms of distribution of phases and residual stresses [15,16]. The stresses are developed during solidification of the alloy due to differential thermal coefficient of expansion of its various microconstituents [15,16]. Heat treatment leads to breaking of the dendritic structure resulting in improved degree of homogeneity of distribution of the microconstituents (except silicon particles and nickel-containing phase) in the alloy microstructure (figure 2(c) versus (a)). The practically unaltered morphology and mode of distribu-

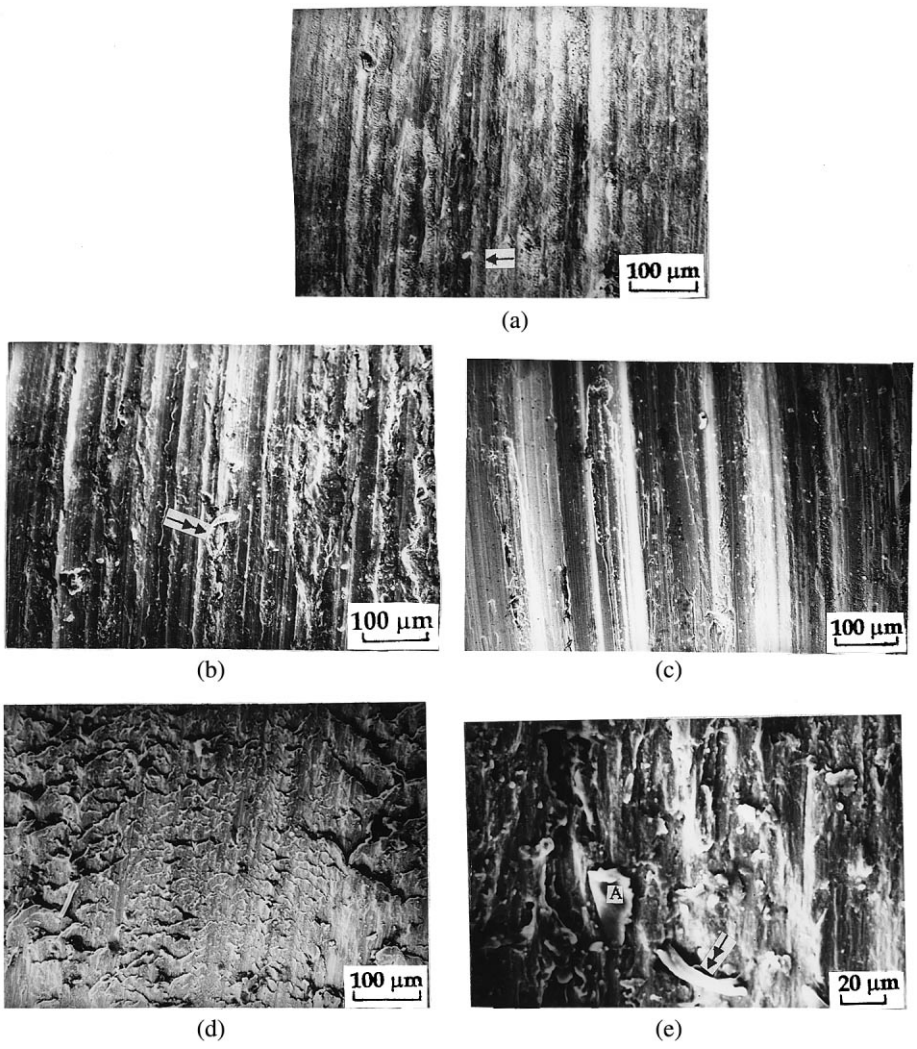

Figure 6. Wear surfaces of the as cast alloy tested at applied pressures of (a and c) 1 MPa, (b) 15 MPa, and (d and e) 9 MPa at sliding speeds of (a and b) 0.42 m/s and (c–e) 4.60 m/s [single arrow: deep grooves; double arrow: machining chips; A: sticking/entrapment of debris].

tion of the silicon particles and nickel-containing phase could be attributed to the low heat treatment (especially solutionizing) temperature prescribed for the (zinc-based) alloy system [16]. Residual stresses are also relieved/reduced during the heat treatment, causing a reduction in hardness [15,16] from 145 HV for the as-cast alloy to 122 HV for the heat-treated one. The various microconstituents of the zinc-based alloy such as α, η, ε, silicon particles and nickel-containing phase have different characteristics and play various roles during sliding wear. The α phase, a solid solution of zinc in aluminium, is deformable in view of its face centred cubic structure [17,18]. The η phase is a solid solution of aluminium in zinc. It has open hexagonal structure with larger c/a ratio than that of an ideal close packed hexagonal structure [19] and hence acts as a solid lubricant [20,21]. The ε phase is an intermetallic compound of copper and zinc and offers wear resistance [22,23]. The nickel-containing phase is an intermetallic compound of nickel and aluminium i.e. $NiAl_3$ [24] having hardness 700–770 HV at temperatures up to 327 °C, which decreases linearly up to 200 HV at 577 °C [25]. The silicon particles also have high hardness (870–1350 HV at temperatures up to 327 °C, reducing to ~300 HV at 627 °C) as reported elsewhere [26]. The nickel and silicon containing phases also offer wear resistance [24] in view of their high hardness even at large operating temperatures [25,26]. The (nickel and silicon containing) phases also enhance the microcracking tendency of the (zinc-based) alloy system, especially at low operating temperatures in view of their poor deformability characteristics [26]. This tendency gets suppressed under high temperature conditions [8,10–14].

Increasing wear rate of the samples with pressure and speed (figure 3) agreed with greater surface damage (figure 6(b) versus (a), 6(d) versus (c), 6(c) versus (a), and 6(d) versus (b)). A reduction in the wear rate of the as-cast samples at 4.60 m/s could be due to suppressed cracking tendency of silicon particles and the nickel-containing phase [8,10–14] in view of the thermal softening of the specimen surface at high operating temperatures, as evident from larger frictional heating at

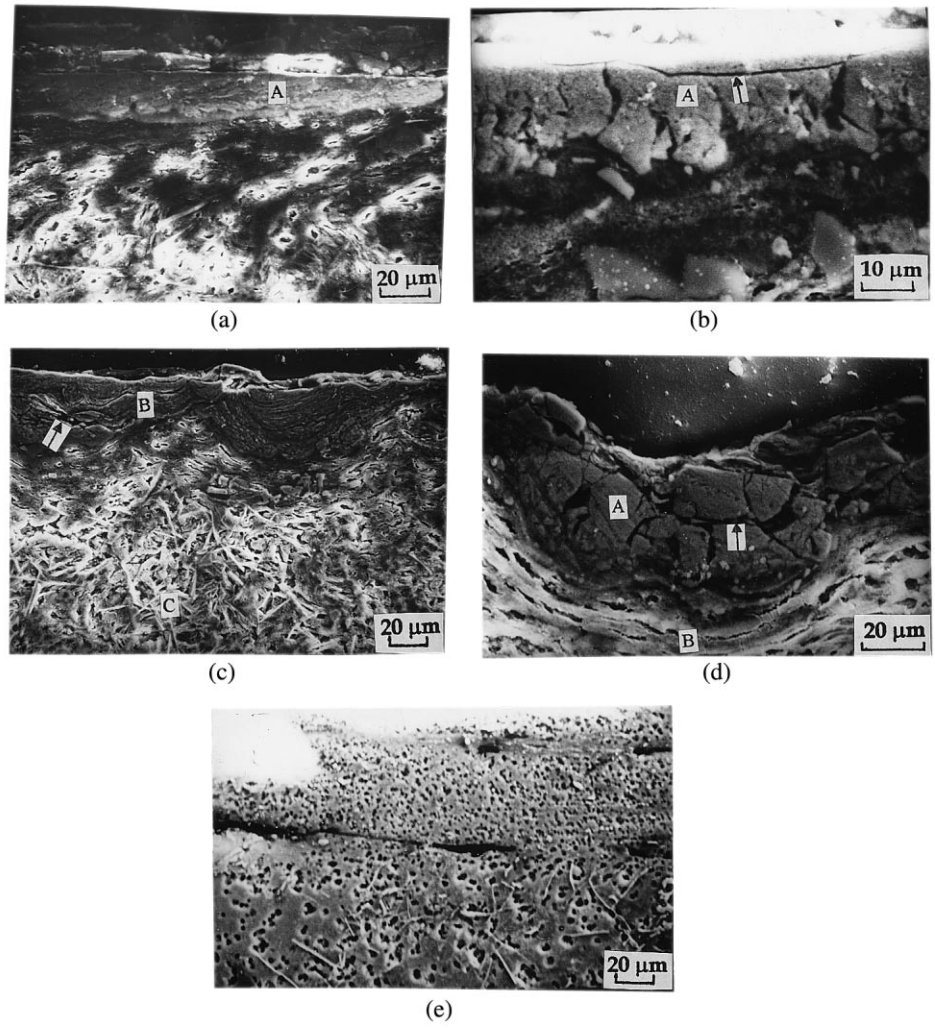

Figure 7. Subsurface regions of the (a–d) as-cast and (e) heat-treated alloy tested at the applied pressures of (a and b) 15 MPa, (c and d) 9 MPa and (e) 6 MPa at sliding speeds of (a and b) 0.42 m/s and (c–e) 4.60 m/s [A: heavily deformed region comprising extremely fine microconstituents; B: flow of microconstituents in sliding direction; C: unaffected bulk structure; arrow: microcracks].

the (higher) sliding speed of 4.60 m/s (figure 5). However, over-softening of the already softened specimen material after heat treatment [15,16] under the circumstances led to deterioration of the wear performance of the alloy through its increased tendency to adhere onto the disc. As a result, the wear rate of the heat-treated alloy increased with speed throughout (figure 3).

The heat-treated samples attained less wear rate than that of the as-cast ones at speeds less than 4.60 m/s (figure 3). This could be attributed to the lesser microcracking tendency of the (softened) alloy after heat treatment than in the as-cast condition [15,16] under low frictional heating at the (low) speeds (figure 4 and 5). The as-cast alloy becomes crack sensitive at low operating temperatures [8,10–14], leading to high wear rate (figure 3). On the contrary, the higher wear rate of the heat-treated alloy over the as-cast one at the sliding speed of 4.60 m/s (figure 3) could be due to the oversoftening of the already softened alloy after heat treatment, causing a high degree of adhesion onto the disc [15,16]. The high frictional heating (figures 4 and 5) under the circumstances further supports this view. This condition, however, was favourable for the as-cast alloy in the sense that the (high) frictional heat could enable one to reduce the severity of its cracking tendency [8,10–14] causing it to perform better (than the heat-treated alloy).

Initially high rate of temperature increase with test duration (figure 4) results from abrasive action on the specimen surface (figure 6(a), region marked by single arrow). The abrasive action is caused by the hard debris particles (figure 8, regions marked by single and double arrows respectively) that get entrapped on the specimen surface (figure 6(b) and (e), regions marked by a double arrow) subsequent upon their release [27]. And such hard (debris) particles (figure 8, regions marked by single and double arrows respectively) emanate as a

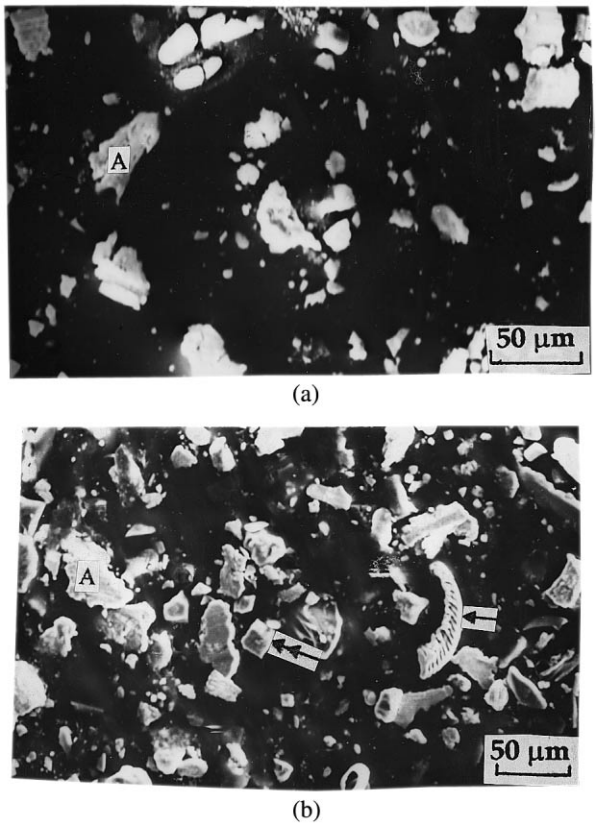

Figure 8. Wear debris of the as-cast alloy after testing at (a) 15 MPa at 0.42 m/s and (b) 9 MPa at 4.60 m/s [A: flaky debris; single arrow: machining chip; double arrow: debris with sharp corners and edges].

result of fragmentation of initially contacting (highly stressed) asperities of the contacting surfaces [28] and hard silicon particles and nickel-containing phase [8,10–14]. With the fragmentation of the asperities, the effective area of contact becomes greater, thereby reducing the severity of stressing [27,28]. Accordingly, the rate of frictional heating decreases at longer test durations (figure 4). A further increase in the rate of frictional heating after attaining the reduced rate of heating could be attributed to the destabilization/rupture of the lubricant film [28,29].

The ripple-like appearance of the wear surface (figure 6(e)) results from stick-slip phenomena when static friction exceeds kinetic friction [30–32]. Varying microstructural features of the specimens with depth below the wear surface in their subsurface regions (figure 7) could be due to the changing severity of wear-induced plastic deformation that the regions undergo [14,24,27–29]. The regions in the nearest vicinity of the wear surface (figure 7, regions marked A) experience the highest severity of deformation and straining [33,34] leading to their extremely fine microconstituents. The regions marked by B in figure 7 (just below the region marked by A) experience relatively less severe deformation leading to the flow of material microconstituents in the sliding direction and fragmentation of the phases. The regions still below the one marked by B in figure 7 undergo no deformation and hence delineate a normal bulk structure (figure 7, regions marked by C) in a manner similar to figure 2. The process of sliding involves accumulation of damage in the wear surface/subsurface regions. Any excessive accumulation of damage/defects makes the regions prone to cracking [35], ultimately leading to their detachment from the bulk and joining the debris subsequently. The presence of microcracks in the subsurface regions (figure 7, arrow-marked regions) further supports this view.

The flaky debris particles (figure 8, regions marked A) are generated by microploughing indicative of plastic deformation (figure 7), while machining chips (figure 8, region marked by single arrow) result from microcutting [36,37]. The debris with sharp corners and edges (figure 8, region marked by double arrow) forms through the fragmentation of the hard microconstituents like the silicon particles and nickel-containing phase (figure 2, regions marked by triple and double arrows respectively) as observed elsewhere [38].

5. Concluding remarks

An appraisal of the observations made in this study suggests that the wear response depends on factors like thermal softening, lubricating characteristics, cracking tendency and mode of distribution of various phases in the alloy. The wear rate increased with pressure for the as-cast and heat-treated alloy samples. This was also substantiated through the increased severity of surface damage. Increasing speed led to higher wear rate of the as-cast alloy up to a sliding speed of 2.68 m/s, while the trend reversed at a still higher speed of 4.60 m/s. The latter was due to the suppressed cracking tendency of the alloy under the conditions of increased operating temperatures at the speed. On the contrary, the heat-treated alloy showed consistently increasing wear rate with speed due to oversoftening of the already softened alloy after heat treatment. Oversoftening increases the tendency of the alloy towards increased degree of adherence of the sample material onto the disc, thereby increasing the probability of material seizure. The heat treatment led to improved wear resistance (inverse of wear rate) up to a specific speed of 2.68 m/s in this study (despite the reduced hardness of the alloy after the treatment) due to improved homogeneity of distribution of various phases and relief of residual stresses therein. This indicates that deterioration in hardness does not always mean inferior wear performance. Moreover, heat treatment needed for dimensional stability could be employed for the variety of zinc-based alloys without sacrificing wear performance, but at the cost of deteriorating mechanical properties like hardness (and strength) within limits.

References

[1] E. Gervais, H. Levert and M. Bess, Trans. AFS 68 (1980) 183.
[2] D. Apelian, M. Paliwal and D.C. Herrschaft, J. Met. 33 (1981) 12.
[3] E.J. Kubel Jr., Adv. Mater. Proc. 132 (1987) 51.
[4] E. Gervais, R.J. Barnhurst and C.A. Loong, J. Met. 37 (1985) 43.
[5] K. Lohberg, Z. Metallkd. 74 (1983) 456.
[6] B.K. Prasad, J. Mater. Eng. Perf. 7 (1998) 632.
[7] B.K. Prasad, A.K. Patwardhan and A.H. Yegneswaran, J. Mater. Sci. Lett. 16 (1997) 1890.
[8] B.K. Prasad, Z. Metallkd. 88 (1997) 929.
[9] B.K. Prasad, Mater. Sci. Eng. A 245A (1998) 257.
[10] B.K. Prasad, A.K. Patwardhan and A.H. Yegneswaran, J. Mater. Eng. Perf. 7 (1998) 130.
[11] B.K. Prasad, Mater. Trans. JIM 38 (1997) 701.
[12] B.K. Prasad, A.K. Patwardhan and A.H. Yegneswaran, Scri. Mater. 37 (1997) 323.
[13] B.K. Prasad, Mater. Charact. 44 (2000) 301.
[14] B.K. Prasad, A.K. Patwardhan and A.H. Yegneswaran, Metall. Mater. Trans. A 27A (1996) 3513.
[15] B.K. Prasad, Mater. Sci. Technol. 13 (1997) 928.
[16] B.K. Prasad, Wear 240 (2000) 100.
[17] G.E. Dieter, ed., *Mechanical Metallurgy*, 2nd Ed. (McGraw-Hill, 1983) p. 105.
[18] S. Murphy and T. Savaskan, Wear 98 (1984) 151.
[19] S.W.K. Morgan, (ed.), *Zinc and Its Alloys and Compounds*, 1st Ed. (Ellis Horwood/John Wiley & Sons, New York, 1985) p. 154.
[20] T. Tsuya and R. Takagi, Wear 7 (1964) 131.
[21] E.R. Braithwaite and G.W. Rowe, Sci. Lubr. (1963) 92.
[22] R.J. Barnhurst and J.C. Farge, *Proc. Int. Conf. Cast Zinc-Aluminium (ZA) Alloys, 25th Annual Conference of Metallurgists*, (eds.) G.P. Lewis, R.J. Barnhurst and C.A. Loong, Metallurgical Society of Canadian Institute of Metals, Toronto, Ontario, Canada, Aug. 17–20, 1986, p. 85.
[23] T.J. Risdon, W.M. Mihaichuk and R.J. Barnhurst, *Proc. Int. Congr. Expo., SAE, Feb. 24–28, 1986*, Detroit, Michigan, Paper No. 860064.
[24] P. Choudhury, S. Das and B.K. Datta, J. Mater. Sci. 37 (2002) 2103.
[25] L.F. Mondolfo, ed., *Aluminium Alloys: Structure and Properties*, 1st Ed. (Butterworth & Co. (Publishers) Ltd., London, 1976) p. 338.
[26] L.F. Mondolfo, ed., *Aluminium Alloys: Structure and Properties*, 1st Ed. (Butterworth & Co. (Publishers) Ltd., London, 1976) p. 368.
[27] O.P. Modi, B.K. Prasad, A.H. Yegneswaran and M.L. Vaidya, Mater. Sci. Eng. A 151A (1992) 235.
[28] B.K. Prasad, A.K. Patwardhan and A.H. Yegnesaran, Mater. Sci. Technol. 12 (1996) 427.
[29] B.K. Prasad, A.K. Patwardhan and A.H. Yegneswaran, Can. Metall. Quart. 40 (2001) 193.
[30] F.P. Bowden and D. Tabor, eds., *The Friction and Wear of Solids* (Clarendon Press, Oxford, 1986).
[31] C. Gao, D.K. Wilsdorf and D.D. Makel, Wear 162 (1993) 1139.
[32] S.L. Zhang and J.M. Valentine, Tribol. Int. 12 (2002) 195.
[33] W.A. Glaeser, Wear, 123 (1998) 155.
[34] J. Larsen-Badse, Scri. Metall. 24 (1990) 821.
[35] N.P. Suh, Wear 44 (1977) 1–16.
[36] S. Das, B.K. Prasad, A.K. Jha, O.P. Modi and A.H. Yegneswaran, Wear 162–164 (1993) 802.
[37] O.P. Modi, B.K. Prasad, S. Das, A.K. Jha and A.H. Yegneswraan, Mater. Trans. JIM 35 (1994) 67.
[38] B.K. Prasad, A.K. Patwardhan and A.H. Yegneswaran, Wear 199 (1996) 142.